

# *Candidatus Nitrosopolaris*, a genus of putative ammonia-oxidizing archaea with a polar/alpine distribution

Igor S. Pessi<sup>1,2</sup>, Aino Rutanen<sup>1</sup>, and Jenni Hultman<sup>1,2,3\*</sup>

<sup>1</sup>Department of Microbiology, University of Helsinki, Helsinki, Finland

<sup>2</sup>Helsinki Institute of Sustainability Science (HELSUS), Helsinki, Finland

<sup>3</sup>Natural Resources Institute Finland (LUKE), Helsinki, Finland

\*Corresponding author: [jenni.hultman@helsinki.fi](mailto:jenni.hultman@helsinki.fi)

## Abstract

Ammonia-oxidizing archaea (AOA) are key players in the nitrogen cycle of polar soils. Here, we analysed metagenomic data from tundra soils in Rásttigáisá, Norway, and recovered four metagenome-assembled genomes (MAGs) assigned to the genus “UBA10452”, an uncultured lineage of putative AOA in the order Nitrososphaerales (“terrestrial group I.1b”), phylum Thaumarchaeota. Analysis of other eight previously reported MAGs and publicly available amplicon sequencing data revealed that the UBA10452 lineage is predominantly found in acidic polar and alpine soils. In particular, UBA10452 MAGs were more abundant in highly oligotrophic environments such as mineral permafrost than in more nutrient-rich, vegetated tundra soils. UBA10452 MAGs harbour multiple copies of genes related to cold tolerance, particularly genes involved in DNA replication and repair. Based on the phylogenetic, biogeographical, and ecological characteristics of 12 UBA10452 MAGs, which include a high-quality MAG (90.8% complete, 3.9% redundant) with a nearly complete 16S rRNA gene, we propose a novel *Candidatus* genus, *Ca. Nitrosopolaris*, with four species representing clear biogeographical/habitat clusters.

## Introduction

Nitrification – the oxidation of ammonia to nitrite and further oxidation to nitrate – is a crucial part of the nitrogen (N) cycle providing a link between reduced and oxidized forms of N. The first step of nitrification, ammonia oxidation, is carried out mainly by aerobic chemolithoautotrophic microorganisms that grow by coupling the energy obtained from the oxidation of ammonia with carbon dioxide (CO<sub>2</sub>) fixation (Lehtovirta-Morley, 2018). Ammonia-oxidizing archaea (AOA) outnumber ammonia-oxidizing bacteria (AOB) by orders of magnitude

30 in many terrestrial and aquatic environments, particularly in oligotrophic environments with  
31 low N input (Leininger *et al.*, 2006; Schleper and Nicol, 2010; Lehtovirta-Morley, 2018). Among  
32 the reasons for their ecological success is an enzymatic machinery with higher affinity for  
33 ammonia and a more efficient CO<sub>2</sub> fixation pathway than their bacterial counterparts (Martens-  
34 Habbena *et al.*, 2009; Könneke *et al.*, 2014; Kerou *et al.*, 2016). However, high ammonia affinity  
35 is not a common trait to all AOA, with some strains displaying a low substrate affinity that is  
36 comparable to that of non-oligotrophic AOB (Kits *et al.*, 2017; Jung *et al.*, 2022).

37 Ammonia oxidation is an important process in polar soils despite commonly N limited and cold  
38 conditions (Alves *et al.*, 2013; Siljanen *et al.*, 2019; Hayashi *et al.*, 2020). AOA generally  
39 outnumber AOB in oligotrophic polar soils and are often represented by few species (Alves *et al.*,  
40 2013; Magalhães *et al.*, 2014; Richter *et al.*, 2014; Pessi *et al.*, 2015, 2022, pre-print; Siljanen  
41 *et al.*, 2019; Ortiz *et al.*, 2020). Due to their predominance, AOA are important contributors to  
42 the N cycle in polar soils and are thus key players in the cycling of the potent greenhouse gas  
43 nitrous oxide (N<sub>2</sub>O). Contrary to earlier assumptions, polar soils are increasingly recognized as  
44 important sources of N<sub>2</sub>O (Voigt *et al.*, 2020). Both the nitrite originated from the oxidation of  
45 ammonia as well as the nitrate produced in the second step of nitrification are the substrates of  
46 denitrification, an anaerobic process that has N<sub>2</sub>O as a gaseous intermediate (Butterbach-Bahl  
47 *et al.*, 2013). Moreover, AOA have been directly implicated in the production of N<sub>2</sub>O under oxic  
48 conditions via several mechanisms such as hydroxylamine oxidation and nitrifier  
49 denitrification (Wu *et al.*, 2020). However, both the direct and indirect role of AOA in the cycling  
50 of N<sub>2</sub>O is much less understood compared to their bacterial counterparts.

51 AOA are notoriously difficult to cultivate and so far only three genera have been formally  
52 described based on axenic cultures: *Nitrosopumilus* (Qin *et al.*, 2017) and *Nitrosarchaeum* (Jung  
53 *et al.*, 2018) in the order Nitrosopumilales (“marine group I.1a”) and *Nitrososphaera*  
54 (Stieglmeier *et al.*, 2014) in the order Nitrososphaerales (“terrestrial group I.1b”). Several  
55 provisional *Candidatus* genera have also been proposed based on non-axenic enrichments, e.g.  
56 *Ca.* Nitrosocaldus (“termophilic group”) (de la Torre *et al.*, 2008) and *Ca.* Nitrosotalea (“group  
57 I.1a-associated”) (Lehtovirta-Morley *et al.*, 2011). Moreover, the growing use of genome-resolved  
58 metagenomics has resulted in the identification of tens of novel, currently uncultured lineages  
59 in the phylum Thaumarchaeota (Rinke *et al.*, 2021). These lineages are phylogenetically distinct  
60 from both formally described and *Candidatus* taxa and are identified with placeholder  
61 alphanumeric identifiers (e.g., the Nitrososphaerales genus “UBA10452”). The identification of  
62 these novel lineages by metagenomics greatly expands our knowledge of the diversity of AOA  
63 but detailed descriptions of their metabolic and ecological features are generally lacking.

64 Recently, we have applied a genome-resolved metagenomics approach to gain insights into the  
65 microorganisms involved with the cycling of greenhouse gases in tundra soils from Kilpisjärvi,  
66 Finland (Pessi *et al.*, 2022, pre-print). Analysis of *amoA* genes encoding the alpha subunit of the  
67 enzyme ammonia monooxygenase (Amo) revealed a very low diversity of ammonia oxidizers,  
68 with only four genes annotated as *amoA* out of 23.5 million assembled genes. Three of these  
69 were most closely related to the *amoA* gene of the comammox bacterium *Ca. Nitrospira*  
70 *inopinata* (Daims *et al.*, 2015). The remaining *amoA* gene was binned into a metagenome-  
71 assembled genome (MAG) assigned to the genus “UBA10452”, an uncharacterized archaeal  
72 lineage in the order Nitrososphaerales, phylum Thaumarchaeota (Rinke *et al.*, 2021). Here, we  
73 i) report four novel UBA10452 MAGs obtained from tundra soils in Rásttigáisá, Norway; ii)  
74 characterize the genomic properties, metabolic potential, phylogeny, and biogeography of the  
75 UBA10452 lineage; and iii) propose the creation of a new *Candidatus* genus, *Ca. Nitrosopolaris*.

## 76 **Methods**

### 77 **Sampling and metagenome sequencing**

78 Ten soil samples were obtained in July 2017 across an area of alpine tundra in Rásttigáisá,  
79 Norway (69°59'N, 26°15'E, 700 m.a.s.l.). DNA was extracted from the mineral layer (10–15 cm  
80 depth) with the PowerSoil DNA Isolation kit (QIAGEN, Venlo, Netherlands) according to the  
81 manufacturer’s instructions. Paired-end metagenomic sequencing was done using the Illumina  
82 NextSeq500 platform (Illumina, San Diego, CA, USA) at the DNA Sequencing and Genomics  
83 Laboratory (Institute of Biotechnology, University of Helsinki).

### 84 **Metagenome assembling and binning**

85 Removal of adapter sequences and low-quality base calls (Phred score < 28) was done with  
86 Cutadapt v1.10 (Martin, 2011) and sequences were assembled with MEGAHIT v1.1.1 setting a  
87 minimum contig length of 1,000 bp (Li *et al.*, 2015). Samples were assembled individually and  
88 as one co-assembly of all samples pooled together. Manual MAG binning was done with anvio  
89 v6.0 (Eren *et al.*, 2015) according to Pessi *et al.* (2022, pre-print). In brief, Prodigal v2.6.3 (Hyatt  
90 *et al.*, 2010) was used to predict gene calls and single-copy genes were identified with HMMER  
91 v.3.2.1 (Eddy, 2011). Bowtie v2.3.5 (Langmead and Salzberg, 2012) and SAMtools v1.9 (Li *et al.*,  
92 2009) were used to map the quality-filtered Illumina reads to the contigs. Contigs were then  
93 manually binned into MAGs based on differential coverage and tetranucleotide frequency using

94 the *anvi-interactive* interface of *anvi'o* v6.0. MAGs were manually inspected and refined using  
95 the *anvi-refine* interface of *anvi'o* v6.0.

## 96 **Metagenome-assembled genomes assigned to the UBA14052 lineage**

97 MAGs were classified based on 122 archaeal and 120 bacterial single-copy genes with GTDB-  
98 Tk v1.3.0 (Chaumeil *et al.*, 2019) and the GTDB release 05-RS95 (Parks *et al.*, 2018, 2020).  
99 MAGs assigned to the genus “UBA10452” in the order Nitrososphaerales (“terrestrial group  
100 I.1b”), phylum Thaumarchaeota (Rinke *et al.*, 2021), were selected for downstream analyses  
101 **(Table 1, Suppl. Table S1)**. In addition, we analysed other eight UBA10452 MAGs available  
102 on GenBank and GTDB release 95 (Parks *et al.*, 2018, 2020). These included six MAGs from  
103 permafrost soil in Canada (Chauhan *et al.*, 2014; Parks *et al.*, 2017), one MAG from polar desert  
104 soil in Antarctica (Ji *et al.*, 2017), and one MAG from tundra soil in Finland (Pessi *et al.*, 2022).

## 105 **Genome annotation**

106 We used *anvi'o* v7.0 (Eren *et al.*, 2015) to predict gene calls with Prodigal v2.6.3 (Hyatt *et al.*,  
107 2010), identify ribosomal genes and a set of 76 archaeal single-copy genes with HMMER v.3.3  
108 (Eddy, 2011), and compute genome completion and redundancy levels based on the presence of  
109 the 76 single-copy genes. We also employed *anvi'o* v7.0 to annotate the gene calls against the  
110 KOfam (Aramaki *et al.*, 2020) and Pfam (Mistry *et al.*, 2021) databases with HMMER v.3.3  
111 (Eddy, 2011) and the COG database (Galperin *et al.*, 2021) with DIAMOND v0.9.14 (Buchfink  
112 *et al.*, 2015). Additionally, we used BLASTP v2.10.1 (Camacho *et al.*, 2009) to annotate the gene  
113 calls against the arCOG database (Makarova *et al.*, 2015). Matches with scores below the pre-  
114 computed family-specific thresholds (KOfam and Pfam), e-value > 10<sup>-6</sup> (COG), or identity < 35%  
115 and coverage < 75% (arCOG) were discarded and, in case of multiple matches, the one with the  
116 lowest e-value was kept.

117 We used BLASTP v2.10.1 to compare the amino acid sequences of genes identified as *amoA*,  
118 *amoB*, or *amoC* to the RefSeq (O’Leary *et al.*, 2016) and Swiss-Prot (The UniProt Consortium,  
119 2019) databases, and BLASTN v2.10.1 (Camacho *et al.*, 2009) to compare *amoA* genes against  
120 the nt database and the curated *amoA* database of Alves *et al.* (2018). Functional enrichment  
121 analyses were carried out using *anvi'o* v7.0 (Eren *et al.*, 2015) according to Shaiber *et al.* (2020).  
122 In brief, the occurrence of arCOG functions across genomes was summarised and logistic  
123 regression was then used to identify functions associated with a particular genus or genera. For  
124 this, we considered only the three most complete *Nitrososphaera*, *Ca. Nitrosocosmicus*, and *Ca.*  
125 *Nitrosodeserticola* genomes plus the representative genome of each *Ca. Nitrosopolaris* species.

126 **Table 1.** List of metagenome-assembled genomes (MAGs) belonging to the UBA10452 lineage  
127 (*Candidatus Nitrosopolaris*).

| 128 | MAG                | Isolation source                                | Accession       | Ref. |
|-----|--------------------|---|-----------------|------|
| 129 | COA_Bin_4_1        | Tundra soil, Rásttigáisá, Norway                | GCA_933227015.1 | [1]  |
| 130 | S89_Bin_2          | Tundra soil, Rásttigáisá, Norway                | GCA_933227005.1 | [1]  |
| 131 | S100_Bin_4         | Tundra soil, Rásttigáisá, Norway                | GCA_933226995.1 | [1]  |
| 132 | S1130_Bin_3        | Tundra soil, Rásttigáisá, Norway                | GCA_933226985.1 | [1]  |
| 133 | KWL-0179           | Tundra soil, Kilpisjärvi, Finland               | GCA_936417005.1 | [2]  |
| 134 | UBA272             | Permafrost soil, Nunavut, Canada                | GCA_002504425.1 | [3]  |
| 135 | UBA273             | Permafrost soil, Nunavut, Canada                | GCA_002501935.1 | [3]  |
| 136 | UBA347             | Permafrost soil (active layer), Nunavut, Canada | GCA_002495965.1 | [3]  |
| 137 | UBA348             | Permafrost soil (active layer), Nunavut, Canada | GCA_002501855.1 | [3]  |
| 138 | UBA466             | Permafrost soil (active layer), Nunavut, Canada | GCA_002498345.1 | [3]  |
| 139 | UBA536             | Permafrost soil (active layer), Nunavut, Canada | GCA_002496625.1 | [3]  |
| 140 | RRmetagenome_bin19 | Polar desert soil, Wilkes Land, Antarctica      | GCA_003176995.1 | [4]  |

141 1. This study.

142 2. Pessi et al. (2022, pre-print).

143 3. Parks et al. (2017), based on data originally published by Chauhan et al. (2014).

144 4. Ji et al. (2017).

## 145 **Phylogenomic and phylogenetic analyses**

146 For phylogenomic analysis, we used a set of 59 archaeal single-copy genes that were present in  
147 at least 80% of the genomes. In addition to the 12 UBA10452 MAGs, we retrieved from GenBank  
148 other 33 genomes belonging to the family Nitrososphaeraceae and the genome of  
149 *Nitrosopumilus maritimus* SCM1 to be used as an outgroup. We used anvi'o v7.0 (Eren *et al.*,  
150 2015) to recover the predicted amino acid sequence for each of the 59 genes, align them  
151 individually with MUSCLE v3.8.1551 (Edgar, 2004), and generate a concatenated alignment.  
152 We then computed a maximum likelihood tree with IQ-TREE v2.1.4 employing the automatic  
153 model selection and 1000 bootstraps (Nguyen *et al.*, 2015). Pairwise average nucleotide identity  
154 (ANI) values were computed with pyani v0.2.10 (Pritchard *et al.*, 2016) and amino acid identity  
155 (AAI) values with the AAI-Matrix tool (<http://enve-omics.ce.gatech.edu/g-matrix>).

156 Phylogenetic analysis of the *amoA* and 16S rRNA genes were done as described for the  
157 phylogenomic analysis (i.e., alignment with MUSCLE and tree building with IQ-TREE). Genes  
158 annotated as multicopper oxidase (PF07731, PF07732, COG2132, or arCOG03914) or nitrite  
159 reductase were aligned with MAFFT v7.490 (Katoh and Standley, 2013) alongside the



160 sequences reported by Kerou *et al.* (2016), and a maximum likelihood tree was computed with  
161 IQ-TREE v2.1.4 (Nguyen *et al.*, 2015) as described above.

## 162 **Abundance and geographic distribution**

163 We employed read recruitment to compute the relative abundance of the UBA10452 lineage  
164 across the metagenomics datasets from which the MAGs were originally recovered. These  
165 datasets consisted of 10 Illumina NextSeq metagenomes from tundra soils in Rásttigáisá,  
166 Norway (this study); 69 Illumina NextSeq/NovaSeq metagenomes from tundra soils in  
167 Kilpisjärvi, Finland (Pessi *et al.*, 2022, pre-print); 13 Illumina HiSeq metagenomes from  
168 permafrost soils in Nunavut, Canada (Chauhan *et al.*, 2014; Stackhouse *et al.*, 2015); and three  
169 Illumina HiSeq metagenomes from polar desert soils in Wilkes Land, Antarctica (Ji *et al.*, 2017).  
170 We used fasterq-dump v2.10.8 (<https://github.com/nbci/sra-tools>) to retrieve the raw  
171 metagenomic data from the Sequence Read Archive (SRA). We then used CoverM v0.6.1  
172 (<https://github.com/wwood/CoverM>) to map the reads to the MAGs with minimap v2.17 (Li,  
173 2016) and to compute relative abundances based on the proportion of reads recruited by the  
174 MAGs. In addition, we used IMNGS (Lagkouravdos *et al.*, 2016) to further investigate the  
175 geographic distribution of the UBA10452 lineage. For this, we used the 16S rRNA gene sequence  
176 of the MAG RRmetagenome\_bin19 as query to screen 422,877 amplicon sequencing datasets in  
177 SRA with UBLAST (Edgar, 2010). We considered only matches with  $\geq 99.0\%$  similarity.

## 178 **Results**

### 179 **Genomic characteristics of the UBA10452 lineage**

180 We applied a genome-resolved metagenomics approach to data obtained from tundra soils in  
181 Rásttigáisá, Norway, and recovered four MAGs assigned to the genus “UBA10452”, an  
182 uncultured lineage in the order Nitrososphaerales (“terrestrial group I.1b”), phylum  
183 Thaumarchaeota (Rinke *et al.*, 2021). The UBA10452 lineage is currently represented by eight  
184 MAGs in GTDB and GenBank in addition to the four MAGs obtained in the present study  
185 **(Table 1, Fig. 1a)**. Genome completion and redundancy estimated with anvi'o v7.0 (Eren *et al.*,  
186 2015) based on the presence of 76 single-copy genes range from 50.0–90.8% and 2.6–9.2%,  
187 respectively **(Fig. 1b, Suppl. Table S1)**. The MAG RRmetagenome\_bin19, with 90.8%  
188 completion, 3.9% redundancy, and a nearly complete (1462 bp) 16S rRNA gene, is a high-quality  
189 MAG according to the MIMAG standard (Bowers *et al.*, 2017). The remaining 11 MAGs are of  
190 medium quality ( $\geq 50\%$  complete,  $< 10\%$  redundant), four of which also include the 16S rRNA

191 gene. The genome size of UBA10452 MAGs ranges from 0.8 Mb (MAG S1130\_Bin\_3, 60.5%  
192 complete) to 4.0 Mb (MAG RRmetagenome\_bin19, 90.8% complete). G+C content ranges from  
193 38.1 to 41.5%.

## 194 **UBA10452 has a predominantly polar distribution**

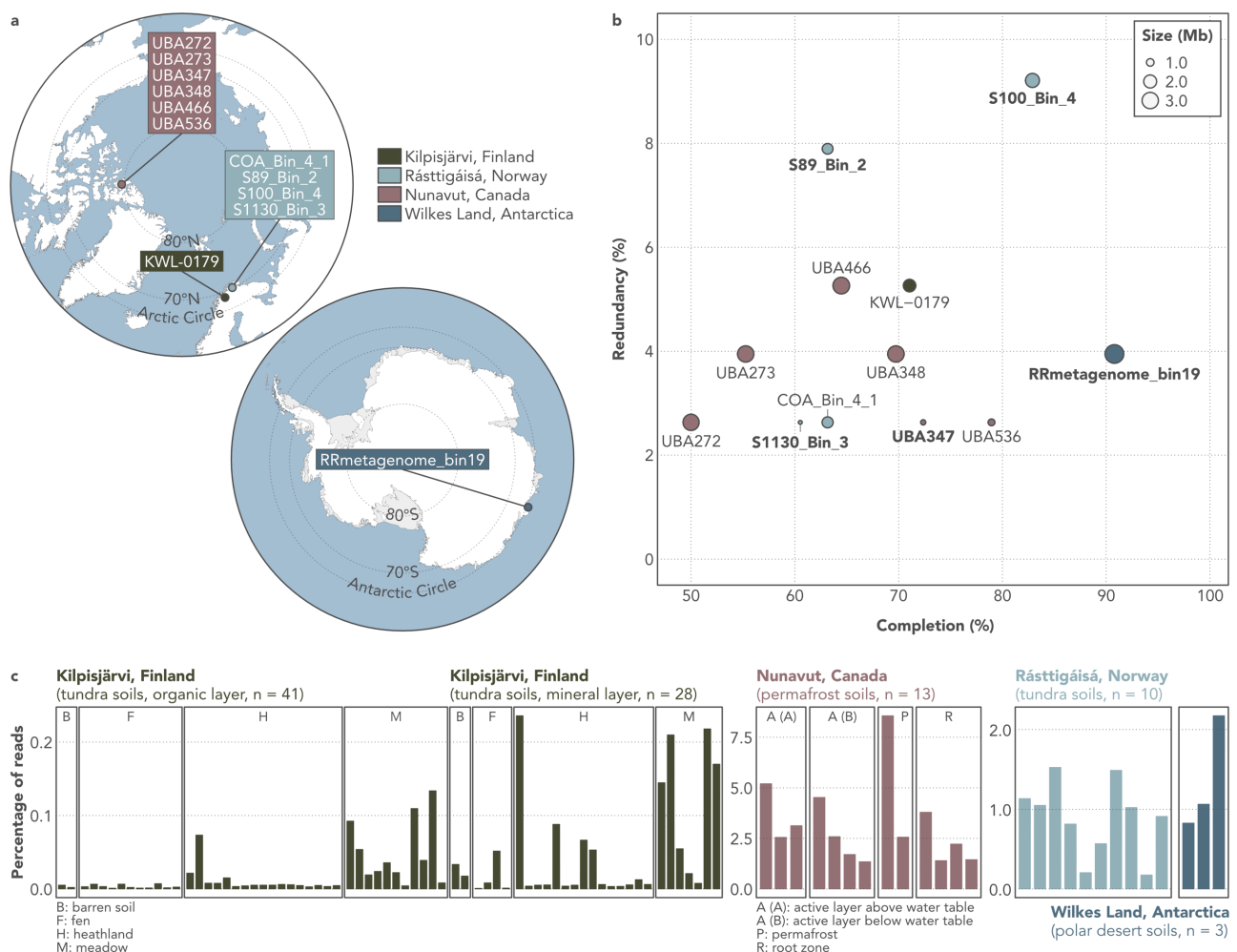
195 All 12 UBA10452 MAGs were obtained from tundra, permafrost, and polar desert soils (**Table**  
196 **1, Fig. 1a**). To gain insights into the ecology of the UBA10452 lineage, we used read recruitment  
197 to quantify the abundance of UBA10452 MAGs in the metagenomic datasets from which they  
198 were assembled. UBA10452 MAGs were most abundant in the dataset of permafrost from  
199 nutrient-poor (C: 1.0%, N: 0.1%) mineral cryosols in Nunavut, Canadian Arctic, where they  
200 recruited up to 8.6% of the reads in each sample (**Fig. 1c**). On the other hand, UBA10452 MAGs  
201 were least abundant in the more nutrient-rich (C: 7.3%, N: 0.3%) tundra soils from Kilpisjärvi,  
202 Finland, where they were detected particularly in samples taken from the mineral layer of  
203 heathland and meadow soils.

204 In order to investigate further the geographic distribution of the UBA10452 lineage, we used  
205 IMNGS (Lagkouvardos *et al.*, 2016) to screen 422,877 16S rRNA gene amplicon sequencing  
206 datasets in SRA. Sequences matching the 16S rRNA gene of UBA10452 MAGs ( $\geq 99.0\%$   
207 similarity) were found across 1281 datasets, mostly consisting of soil ( $n = 750$ ), freshwater ( $n =$   
208  $104$ ), and rhizosphere samples ( $n = 100$ ). Matched reads accounted for 6.0% of the total number  
209 of reads in these datasets (8.9 out of 149.1 million sequences). Of these, the overwhelming  
210 majority (8.7 million reads, 97.9%) come from Antarctic soil datasets, particularly from 149 sites  
211 in the vicinity of Davis Station, Princess Elizabeth Land (Bissett *et al.*, 2016) (**Suppl. Fig. S1a**).  
212 The proportion of reads matching the UBA10452 lineage was above 50% of the archaeal 16S  
213 rRNA gene sequences in 70 of these sites and reached values as high as 88.8% (**Suppl. Fig.**  
214 **S1b**).

## 215 **UBA10452 is a distinct lineage in the family Nitrososphaeraceae**

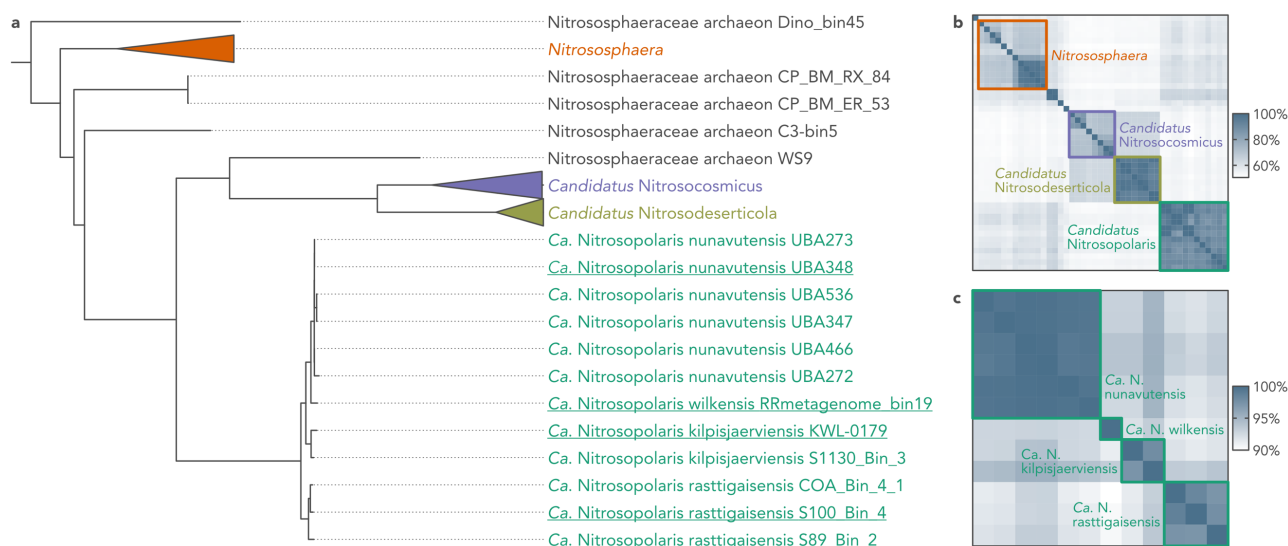
216 Phylogenomic analysis based on 59 single-copy genes placed the UBA10452 MAGs as a distinct  
217 lineage outside *Nitrososphaera*, *Ca. Nitrosocosmicus*, and *Ca. Nitrosodeserticola*, the three  
218 described genera in the family Nitrososphaeraceae (Stieglmeier *et al.*, 2014; Lehtovirta-Morley  
219 *et al.*, 2016; Hwang *et al.*, 2021) (**Fig. 2a; Suppl. Fig. S2**). Separation of UBA10452 is also  
220 supported by AAI and 16S rRNA gene analyses. UBA10452 MAGs share  $59.1\% \pm 1.9$ ,  $53.0\% \pm$   
221  $1.1$ , and  $53.8\% \pm 0.9$  AAI with *Nitrososphaera*, *Ca. Nitrosocosmicus*, and *Ca. Nitrosodeserticola*,  
222 respectively (**Fig. 2b**), all of which are below the 65% AAI threshold commonly used to delineate

223 microbial genera (Konstantinidis *et al.*, 2017). At the 16S rRNA gene level, UBA10452 MAGs  
 224 are  $94.8\% \pm 1.2$  and  $95.4\% \pm 0.2$  similar to *Nitrososphaera* and *Ca. Nitrosocosmicus*, respectively  
 225 (**Suppl. Fig. S3**). These values are in the limit of the 95% threshold for genus delineation  
 226 proposed by Rosselló-Móra and Amann (2015), but are well below the median 16S rRNA gene  
 227 similarity observed between related genera across different microbial phyla (96.4%; Yarza *et al.*,  
 228 2014). Comparison with *Ca. Nitrosodeserticola* was not possible due to the lack of a 16S rRNA  
 229 gene sequence from this genus. Given that UBA10452 represents a clear, distinct lineage in the  
 230 family Nitrososphaeraceae, we consider that UBA10452 should be recognized as a *Candidatus*  
 231 genus and propose the name *Ca. Nitrosopolaris*.



232 **Figure 1. Geographic origin, assembly statistics, and abundance of metagenome-assembled**  
 233 **genomes (MAGs) assigned to the UBA10452 lineage (*Candidatus Nitrosopolaris*).**  
 234 **a)** Maps of the Arctic and Antarctic regions showing the geographic origin of the 12 UBA10452 MAGs.  
 235 **b)** Genome completion, redundancy, and size of the UBA10452 MAGs. Completion and redundancy levels  
 236 were computed based on the presence of 76 single-copy genes. MAGs in bold include the 16S rRNA gene.  
 237 **c)** Proportion of metagenomic reads recruited by the UBA10452 MAGs across the four datasets from  
 238 which they were originally recovered.





239 **Figure 2. Phylogenomic analysis of the UBA10452 lineage (*Candidatus Nitrosopolaris*).** a)  
 240 Maximum likelihood tree based on 59 single-copy genes from 12 metagenome-assembled genomes (MAGs)  
 241 assigned to the UBA10452 lineage and 33 other Nitrososphaeraceae genomes available on GenBank. The  
 242 tree was rooted with *Nitrosopumilus maritimus* SCM1 (not shown). Representatives for the four proposed  
 243 species are indicated in underscore. An uncollapsed and bootstrapped version of the tree can be found in  
 244 **Suppl. Fig. S2.** b) Pairwise average amino acid identity (AAI) between Nitrososphaeraceae genomes and  
 245 c) average nucleotide identity (ANI) between UBA10452 MAGs. The boxes encompass the four described  
 246 Nitrososphaeraceae genera (AAI threshold of 65%; panel b) and the four proposed species of *Candidatus*  
 247 *Nitrosopolaris* (ANI threshold of 95–96%; panel c). Rows and columns are ordered from top to bottom and  
 248 left to right, respectively, according to the top-bottom order of leaves in panel a.

249 Pairwise ANI values between *Ca. Nitrosopolaris* MAGs range from 90.9 to 99.9% (**Fig. 2c**).  
 250 Based on either a 95% (Konstantinidis *et al.*, 2017) or 96% ANI threshold (Ciuffo *et al.*, 2018),  
 251 the 12 *Ca. Nitrosopolaris* MAGs can be separated into four distinct species (**Fig. 2a**; **Suppl.**  
 252 **Fig. S2**). Two of these, one comprising the six Canadian MAGs (Chauhan *et al.*, 2014; Parks *et*  
 253 *al.*, 2017) and the other consisting solely of the Antarctic MAG (Ji *et al.*, 2017), correspond to  
 254 the two existing species in GTDB release 95 (“UBA10452 sp002501855” and “UBA10452  
 255 sp003176995”, respectively). Here we suggest renaming these species as *Ca. Nitrosopolaris*  
 256 *nunavutensis* and *Ca. Nitrosopolaris wilkensis*, respectively, according to the geographic origin  
 257 of the MAGs. The Finnish MAG (Pessi *et al.*, 2022, pre-print) plus one of the Norwegian MAGs  
 258 obtained in the present study (S1130\_Bin\_3) represent a novel species, for which we suggest the  
 259 name *Ca. Nitrosopolaris kilpisjaerviensiensis*. Finally, the three remaining MAGs obtained in the  
 260 present study (COA\_Bin\_4\_1, S89\_Bin\_2, and S100\_Bin\_4) correspond to another novel species,  
 261 which we propose to be named as *Ca. Nitrosopolaris rasttigaisensis*. However, the separation of  
 262 *Ca. Nitrosopolaris* into four species is not supported by the analysis of the 16S rRNA gene  
 263 (**Suppl. Fig. S3**). The pairwise similarity between 16S rRNA gene sequences across the four

264 ANI clusters range from 99.5 to 99.9%, which is above the 98.7–99.0% threshold commonly used  
265 for species delineation (Stackebrandt and Ebers, 2006; Kim *et al.*, 2014).

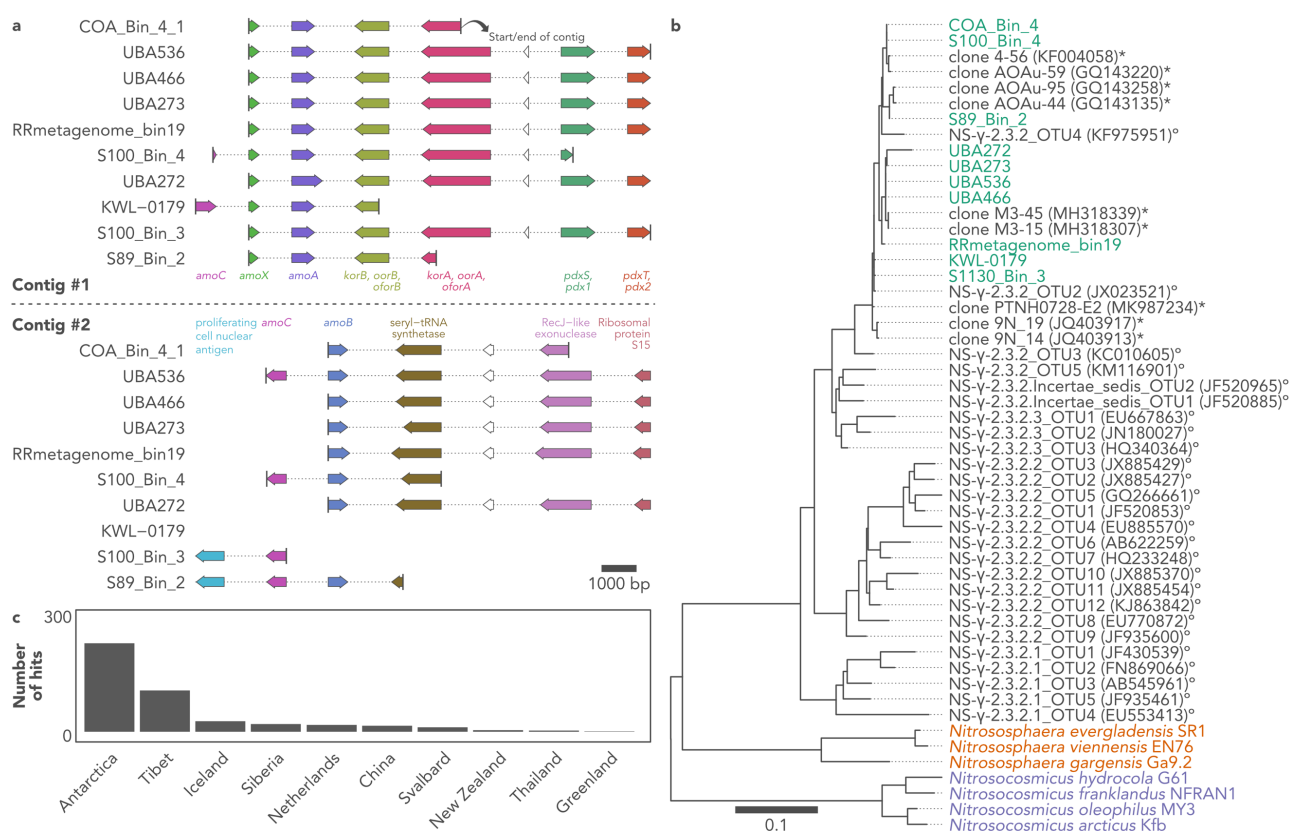
### 266 ***Ca. Nitrosopolaris* harbours genes for ammonia oxidation, CO<sub>2</sub> fixation, and** 267 **carbohydrate metabolism and transport**

268 Annotation of protein-coding genes revealed that *Ca. Nitrosopolaris* harbours the *amoA*, *amoB*,  
269 *amoC*, and *amoX* genes encoding the enzyme ammonia monooxygenase (Amo) which catalyses  
270 the oxidation of ammonia to hydroxylamine (**Fig. 3a, Suppl. Fig. S4, Suppl. Table S2**). As for  
271 other AOA, homologues of the *hao* gene were not found in the *Ca. Nitrosopolaris* MAGs. In AOB,  
272 this gene encodes the enzyme hydroxylamine dehydrogenase (Hao) which takes part in the  
273 oxidation of hydroxylamine to nitrite, a mechanism that remains unknown in AOA (Lehtovirta-  
274 Morley, 2018). A proposed mechanism of hydroxylamine oxidation in AOA is via a copper-  
275 containing nitrite reductase (NirK) encoded by the *nirK* gene, which has been detected in most  
276 *Ca. Nitrosopolaris* MAGs as well as other related multicopper oxidases (**Suppl. Fig. S4**). *Ca.*  
277 *Nitrosopolaris* also encodes an ammonium transporter of the Amt family involved in the uptake  
278 of extracellular ammonium. Moreover, *Ca. Nitrosopolaris* harbours urease (*ureABC*) and urea  
279 transporter (*utp*) genes, indicating the ability to generate ammonia from urea. In contrast to  
280 *Nitrososphaera gargensis* (Spang *et al.*, 2012), we did not detect the *cynS* gene encoding the  
281 enzyme cyanate hydratase involved in the production of ammonia from cyanate.

282 The *amo* genes in all *Ca. Nitrosopolaris* MAGs are distributed across two separate contigs (**Fig.**  
283 **3a**). One of the contigs contains the *amoC*, *amoX*, and *amoA* genes; however, the *amoC* gene is  
284 truncated and found in only two MAGs. In some MAGs, the other contig contains a second, full-  
285 length copy of the *amoC* gene followed by *amoB*. Not all MAGs contain all *amoABCX* genes.  
286 However, considering that the MAGs present varying levels of completion (**Fig. 1b, Suppl.**  
287 **Table S1**) and since the localization of the genes corresponds to start or end of contigs (**Fig.**  
288 **3a**), it is likely that missing genes are an artifact of truncated assemblies rather than due to  
289 gene loss. The *amoA* gene of *Ca. Nitrosopolaris* has a length of 651 bp and belongs to the NS- $\gamma$ -  
290 2.3.2 cluster of Alves *et al.* (2018) (**Fig. 3b**). One exception is the MAG UBA272 which contains  
291 a longer *amoA* gene (873 bp) with a long insert of ambiguous base calls, most likely an artifact  
292 from assembling and/or scaffolding. Sequences belonging to the NS- $\gamma$ -2.3.2 cluster are found  
293 majorly in acidic soils (Alves *et al.*, 2018). Moreover, analysis of sequences from GenBank  
294 showed that the *amoA* gene of *Ca. Nitrosopolaris* is related ( $\geq 96\%$  nucleotide similarity) to  
295 sequences recovered mostly from cold environments, i.e., the Arctic, Antarctica, and alpine  
296 regions such as the Tibetan Plateau (**Fig. 3c**). Among these, the *amoA* sequences of *Ca.*

297 Nitrosopolaris MAGs are most closely related (98.9–99.7% nucleotide similarity) to uncultured  
 298 sequences from Antarctic soil (MH318339 and MH318307), grassland soil in Iceland (JQ403917  
 299 and JQ403913), and the Tibetan Plateau (GQ143258, GQ143220, GQ143135, KF004058, and  
 300 MK987234) (Daebeler *et al.*, 2012; Xie *et al.*, 2014; Wang *et al.*, 2019; Zhang *et al.*, 2019) (**Fig.**  
 301 **3b**).

302 Similarly to other AOA, *Ca. Nitrosopolaris* harbours genes for the hydroxypropionate-  
 303 hydroxybutyrate pathway of CO<sub>2</sub> fixation, complexes I–V of the electron transfer chain, the  
 304 citric acid cycle, and gluconeogenesis (**Suppl. Fig. S4, Suppl. Table S2**). Like other AOA, the  
 305 gene content of *Ca. Nitrosopolaris* indicates a potential for mixotrophic metabolism, with  
 306 multiple copies of genes encoding proteins involved in carbohydrate metabolism and transport  
 307 such as glucose/sorbose dehydrogenases, permeases of the major facilitator superfamily  
 308 (MFS), and pyruvate oxidases. In contrast to *Nitrososphaera*, we did not detect genes involved  
 309 in the assembly of pili, flagellar apparatus (archaellum), and chemotaxis.

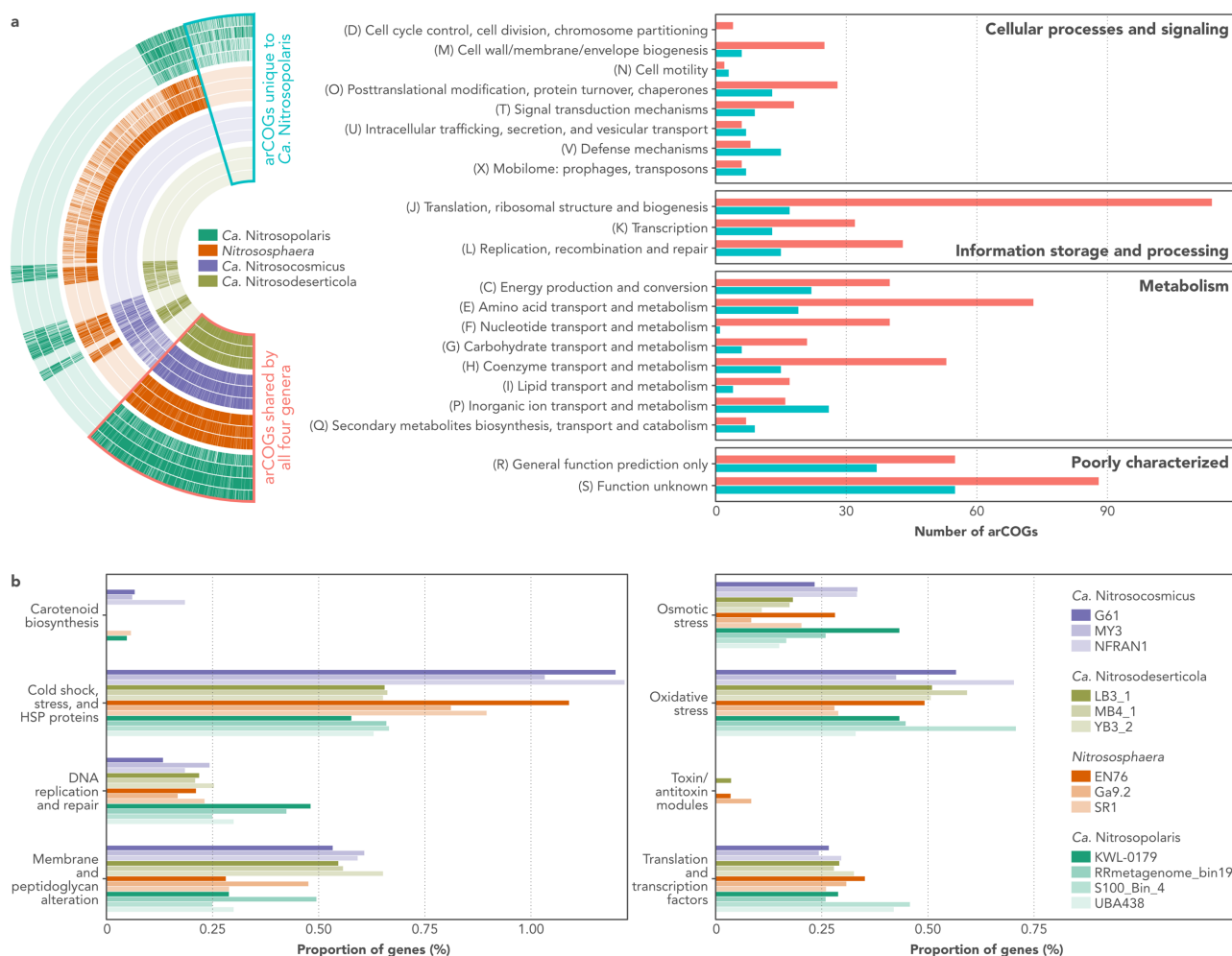


311 **Figure 3. The ammonia monooxygenase (*amo*) genes of UBA10452 (*Candidatus***  
 312 **Nitrosopolaris).** **a)** Representation of two contigs containing *amo* genes in metagenome-assembled  
 313 genomes (MAGs) assigned to the UBA10452 lineage. Two MAGs which do not contain the *amoA* gene are  
 314 omitted (UBA347 and UBA348). **b)** Maximum likelihood tree of the *amoA* sequence of UBA10452 MAGs  
 315 and related sequences from GenBank (asterisks) and Alves *et al.* (2018) (circles). **c)** Geographic origin of  
 316 sequences from GenBank with  $\geq 96.0\%$  nucleotide similarity to the *amoA* sequence of UBA10452 MAGs.

## 317 ***Ca. Nitrosopolaris* MAGs are enriched in genes involved in DNA replication** 318 **and repair**

319 To investigate possible mechanisms underlying the distribution of *Ca. Nitrosopolaris*, we  
320 carried out a functional enrichment analysis covering the four Nitrososphaeraceae genera. In  
321 total, the 13 MAGs used in the analysis encoded 3,999 different arCOG functions (**Fig. 4a**). Of  
322 these, 948 functions were shared among all four genera and 368 were unique to *Ca.*  
323 *Nitrosopolaris*. Of the arCOG functions shared by all four genera, most belonged to the arCOG  
324 classes translation, ribosomal structure, and biogenesis (n = 114), function unknown (n = 88),  
325 and amino acid transport and metabolism (n = 73). On the other hand, arCOG functions unique  
326 to *Ca. Nitrosopolaris* belonged mostly to the arCOG classes function unknown (n = 59), general  
327 function prediction only (n = 52), and inorganic ion transport and metabolism (n = 33). Among  
328 these arCOG functions are several types of hydrolases, lipoproteins, phospholipases, and ABC  
329 transporters including ones for iron, maltose, phosphate, amino acids, and nucleosides (**Suppl.**  
330 **Table S3**).

331 In addition to the genome-wide functional enrichment analysis, we also looked more specifically  
332 for genes with known or predicted roles in cold adaptation and growth (Raymond-Bouchard *et*  
333 *al.*, 2018). When comparing the genomic repertoire of *Ca. Nitrosopolaris* to the other  
334 Nitrososphaeraceae genera, the former was found to harbour a higher number of genes involved  
335 in DNA replication and repair (**Fig. 4b**). More specifically, *Ca. Nitrosopolaris* MAGs encode  
336 multiple copies of the enzymes RecA ATPases and RecA/RadA recombinases (**Suppl. Table S4**).  
337 Surprisingly, genes related to cold shock response were less abundant in *Ca. Nitrosopolaris*  
338 compared to *Nitrososphaera* and *Ca. Nitrosocosmicus* (**Fig. 4b**), although several copies of  
339 molecular chaperones (DnaK, GrpE, and IbpA) and universal stress proteins (UspA) were  
340 identified (**Suppl. Table S4**). In addition to these, *Ca. Nitrosopolaris* also harbours several  
341 copies of other genes encoding proteins related to cold adaptation and growth (**Fig. 4b**),  
342 including proteins involved in membrane and peptidoglycan alteration (glycosyltransferases),  
343 osmotic stress (sodium-hydrogen antiporters and sodium-proline symporters), oxidative stress  
344 (periredoxins and thioredoxin reductases), and translation/transcription (DNA/RNA helicases  
345 and transcription factors) (**Suppl. Table S4**).



346

347 **Figure 4. Comparative genomics of the UBA10452 lineage (*Candidatus Nitrosopolaris*) and**  
 348 **other members of the family Nitrososphaeraceae. a)** Functional enrichment analysis showing  
 349 arCOG functions shared by all Nitrososphaeraceae genera and other functions unique to *Ca.*  
 350 *Nitrosopolaris*. More detail on the arCOG functions unique to *Ca. Nitrosopolaris* can be found in **Suppl.**  
 351 **Table S3. b)** Distribution of genes with known or predicted roles in cold adaptation and growth  
 352 (Raymond-Bouchard *et al.*, 2018). Number of genes is shown as a proportion of the total number of genes  
 353 in each genome. More detail on the genes found in *Ca. Nitrosopolaris* can be found in **Suppl. Table S4.**

## 354 Discussion

355 Genome-resolved metagenomics has revolutionized our knowledge of archaeal diversity by  
 356 giving us access to the genome of uncultured microorganisms at an unprecedented rate (Tahon  
 357 *et al.*, 2021). In a recent metagenomic investigation of tundra soils in northern Finland (Pessi  
 358 *et al.*, 2022, pre-print), we have manually binned and curated a MAG belonging to the genus  
 359 “UBA10452”, an uncultured and largely uncharacterized lineage in the order Nitrososphaerales  
 360 (“terrestrial group I.1b”) of the phylum Thaumarchaeota (Rinke *et al.*, 2021). Here, we binned  
 361 four other UBA10452 MAGs from tundra soils in Rásttigáisá, Norway, and characterized the  
 362 phylogeny, metabolic potential, and biogeography of this lineage. Our results indicate that the



363 UBA10452 lineage consists of putative AOA with a geographic distribution mostly restricted to  
364 cold ecosystems, particularly the polar regions. We suggest the recognition of UBA10452 as a  
365 *Candidatus* genus, for which we propose the name *Ca. Nitrosopolaris* (*nitrosus*: Latin adjective  
366 meaning nitrous; *polaris*: Latin adjective meaning of or pertaining to the poles).

367 The findings from our polyphasic analysis consisting of phylogenomic, AAI, and 16S rRNA gene  
368 analyses support the placement of *Ca. Nitrosopolaris* outside *Nitrososphaera*, *Ca.*  
369 *Nitrosocosmicus*, and *Ca. Nitrosodeserticola* in the family Nitrososphaeraceae, as previously  
370 suggested (Rinke *et al.*, 2021). Our results further indicate that the 12 *Ca. Nitrosopolaris* MAGs  
371 represent four different species based on a 95–96% ANI threshold (Konstantinidis *et al.*, 2017;  
372 Ciufu *et al.*, 2018). In addition to the two current species in GTDB release 95 (Parks *et al.*, 2018,  
373 2020), the inclusion of the four MAGs obtained in the present study resulted in the identification  
374 of two novel species. It is important to note that the separation of *Ca. Nitrosopolaris* into four  
375 species based on ANI values is not readily supported by the analysis of 16S rRNA gene  
376 sequences, which are  $\geq 99.5\%$  similar across the four species. Although a 98.7–99.0% threshold  
377 is commonly used (Stackebrandt and Ebers, 2006), species delineation based solely on the 16S  
378 rRNA gene can be problematic given that microorganisms belonging to different species can  
379 share identical 16S rRNA gene sequences (Kim *et al.*, 2014; Schloss, 2021). One example of this  
380 is *Ca. Nitrosocosmicus arcticus* and *Ca. Nitrosocosmicus oleophilus*, two species of AOA which  
381 share an identical 16S rRNA gene sequence despite having divergent genomes with only 83.0%  
382 ANI (Alves *et al.*, 2019). It thus appears reasonable to conclude that the 12 *Ca. Nitrosopolaris*  
383 MAGs indeed represent four different species as suggested by the ANI analysis. If cultured  
384 representatives become available in the future, phenotypic and ecophysiological  
385 characterization of these isolates could help resolve the taxonomy of *Ca. Nitrosopolaris*.

386 *Ca. Nitrosopolaris* harbours the complete set of *amoA* genes responsible for chemolithotrophic  
387 growth via ammonia oxidation (Lehtovirta-Morley, 2018). Although *in silico* analyses provide  
388 valuable predictions, metabolic capabilities inferred by genomic annotation need to be  
389 confirmed based on the analysis of isolated/enriched cultures or with the help of other indirect  
390 methods such as stable isotope probing (SIP) (Gadkari *et al.*, 2020). Nevertheless, the putative  
391 ammonia oxidation capability of *Ca. Nitrosopolaris* is supported by its close phylogenetic  
392 relationship to *Nitrososphaera* and *Ca. Nitrosocosmicus*, two genera which have been  
393 demonstrated to grow by oxidizing ammonia (Stieglmeier *et al.*, 2014; Lehtovirta-Morley *et al.*,  
394 2016). In addition, the presence of several genes involved in carbohydrate and amino acid  
395 transport and metabolism suggest that *Ca. Nitrosopolaris*, like other AOA, might be able to  
396 grow mixotrophically using organic compounds as alternative energy and/or C sources  
397 (Mussmann *et al.*, 2011; Pester *et al.*, 2011).

398 In addition to the geographical origin of the MAGs, large-scale screening of 16S rRNA gene and  
399 *amoA* sequences from SRA and GenBank indicate that *Ca. Nitrosopolaris* is restricted to soils  
400 in the cold biosphere. The soils from which the *Ca. Nitrosopolaris* MAGs have been recovered  
401 are typical of polar and alpine environments, being characterized by low pH (4.8–5.1), carbon  
402 (C) (1.0–7.3%), and N (0.1–0.3%) content (Stackhouse *et al.*, 2015; Ji *et al.*, 2017; Pessi *et al.*,  
403 2022, pre-print). Furthermore, the abundance profile of *Ca. Nitrosopolaris* observed in this  
404 study, which was characterized by a higher abundance in mineral cryosoil permafrost and polar  
405 desert soils compared to vegetated tundra soils, indicates that *Ca. Nitrosopolaris* is particularly  
406 adapted to the highly oligotrophic conditions found in some of the most extreme environments  
407 in the cryosphere. The discovery of *Ca. Nitrosopolaris* complements the list of microbial taxa  
408 that appear to be adapted to life in cold environments, such as the mat-forming cyanobacteria  
409 *Phormidesmis priestleyi* (Komárek *et al.*, 2009) and *Shackeltoniella antarctica* (Strunecky *et al.*,  
410 2020) and the sea-ice bacteria *Polaribacter* and *Psychrobacter* (Bowman, 2013).

411 Investigation of the genome of *Ca. Nitrosopolaris* provided insights on possible adaptations to  
412 cold and oligotrophic environments. For instance, *Ca. Nitrosopolaris* harbour multiple copies of  
413 several genes that have been implicated in tolerance to cold, such as genes encoding proteins  
414 involved in DNA replication and repair, molecular chaperones, DNA/RNA helicases, and  
415 universal stress proteins (Raymond-Bouchard *et al.*, 2018). Interestingly, *Ca. Nitrosopolaris*  
416 appears to be enriched in copies of the RecA enzyme compared to other members of the  
417 Nitrososphaeraceae. RecA plays a key role in DNA repair, which is an important mechanism  
418 for survival in polar environments where DNA is frequently damaged due to freezing and UV  
419 radiation (Cavicchioli, 2006). In addition to the possible adaptive mechanisms of *Ca.*  
420 *Nitrosopolaris*, it has been suggested that the environmental characteristics of polar soils favour  
421 AOA in general (Alves *et al.*, 2013; Siljanen *et al.*, 2019). The ecological success of AOA in  
422 oligotrophic and acidic soils has been traditionally linked to the higher affinity of their ammonia  
423 oxidation machinery compared to their bacterial counterparts (Martens-Habbena *et al.*, 2009;  
424 Kerou *et al.*, 2016), although a recent study has shown that high affinity for ammonia is not  
425 common to all AOA (Jung *et al.*, 2022). Furthermore, the hydroxypropionate-hydroxybutylate  
426 pathway of CO<sub>2</sub> fixation encoded by *Ca. Nitrosopolaris* and other AOA appears to be more  
427 energy efficient than the Calvin cycle employed by AOB (Könneke *et al.*, 2014). However, these  
428 traits are shared between *Ca. Nitrosopolaris* and other AOA and thus do not readily explain the  
429 apparent ecological success of *Ca. Nitrosopolaris* in cold environments. Indeed, mechanisms of  
430 cold adaptation are evolutionary and functionally complex and involve many features that  
431 cannot be observed by metagenomics alone (e.g., gene regulation and membrane modifications)

432 (Cavicchioli, 2006). Structural, transcriptomics, and proteomics analysis of cultured isolates  
433 could help shed further light on possible adaptations to cold in *Ca. Nitrosopolaris*.

434 In addition to possible mechanisms of adaptation to polar environments, we hypothesize that  
435 the distribution of *Ca. Nitrosopolaris* could be, to some extent, related to historical factors.  
436 Interestingly, the four proposed *Ca. Nitrosopolaris* species form coherent biogeographical  
437 clusters: *Ca. N. nunavutensis*, comprising MAGs obtained from permafrost soils in Nunavut,  
438 Canada; *Ca. N. wilkensis*, corresponding to one MAG from polar desert soils in Wilkes Land,  
439 Antarctica; and *Ca. N. kilpisjaerviensis* and *Ca. N. rasttigaisensis*, comprising MAGs obtained  
440 from mineral tundra soils in two relatively close regions in northern Fennoscandia (Kilpisjärvi  
441 and Rásttigáisá, respectively). A recent molecular dating study has suggested that the origin of  
442 the AOA clade group I.1b (order Nitrososphaerales) coincides with severe glaciation events that  
443 happened during the Neoproterozoic (Yang *et al.*, 2021). If these estimates are accurate, it would  
444 imply that *Ca. Nitrosopolaris* and all other lineages in group I.1b share a common ancestor that  
445 appeared when the global climate was characterized by sub-zero temperatures, having likely  
446 evolved at glacial refugia such as nunataks or regions with geothermal activity.

447 Due to low temperatures throughout the year, polar soils store a large amount of organic matter  
448 and have thus served as important carbon sinks. At present, polar soils are considered minor  
449 yet significant sources of N<sub>2</sub>O (Voigt *et al.*, 2020) but, if warming trends continue at the levels  
450 observed currently, polar soils might become major contributors to the global N<sub>2</sub>O budget. For  
451 instance, the AOA *Ca. Nitrosocosmicus arcticus* isolated from Arctic soil has an ammonia  
452 oxidation optimum at temperatures well above those found *in situ* (Alves *et al.*, 2019). Given  
453 that both the direct and indirect roles of AOA in the cycling of N<sub>2</sub>O in polar soils remain largely  
454 undetermined, a better understanding of polar microbial communities is paramount to model  
455 current and future N<sub>2</sub>O fluxes from this biome.

## 456 **Acknowledgments**

457 This study was funded by the Academy of Finland (project 335354) and the University of  
458 Helsinki. We would like to acknowledge the CSC – IT Centre for Science, Finland, for providing  
459 computing resources; Miska Luoto and the BioGeoClimate Modelling Lab at the University of  
460 Helsinki for providing the Rásttigáisá samples; Eeva Eronen-Rasimus, Laura Cappelatti, and  
461 Benoit Durieu for helpful suggestions and discussions; and Jouko Rikkinen and Heino Vänskä  
462 for nomenclatural advice.

## 463 **Data availability**

464 Genomic assemblies can be found in GenBank/ENA under the accession numbers listed in  
465 **Table 1**. MAGs generated in this study have been submitted to ENA (BioProject PRJEB49283).  
466 All the code used can be found in [https://github.com/ArcticMicrobialEcology/candidatus-](https://github.com/ArcticMicrobialEcology/candidatus-nitrosopolaris)  
467 [nitrosopolaris](https://github.com/ArcticMicrobialEcology/candidatus-nitrosopolaris).

## 468 **Author contributions**

469 ISP, AR, and JH designed the study. ISP performed the analyses and wrote the manuscript. AR  
470 and JH revised the manuscript.

## 471 **Competing interests**

472 The authors declare no conflict of interests.

## 473 **References**

- 474 Alves, R.J.E., Kerou, M., Zappe, A., Bittner, R., Abby, S.S., Schmidt, H.A., et al. (2019) Ammonia  
475 Oxidation by the Arctic Terrestrial Thaumarchaeote Candidatus Nitrosocosmicus arcticus Is  
476 Stimulated by Increasing Temperatures. *Front Microbiol* **10**: 1571.
- 477 Alves, R.J.E., Minh, B.Q., Urich, T., von Haeseler, A., and Schleper, C. (2018) Unifying the  
478 global phylogeny and environmental distribution of ammonia-oxidising archaea based on amoA  
479 genes. *Nat Commun* **9**: 1517.
- 480 Alves, R.J.E., Wanek, W., Zappe, A., Richter, A., Svenning, M.M., Schleper, C., and Urich, T.  
481 (2013) Nitrification rates in Arctic soils are associated with functionally distinct populations of  
482 ammonia-oxidizing archaea. *ISME J* **7**: 1620–1631.
- 483 Aramaki, T., Blanc-Mathieu, R., Endo, H., Ohkubo, K., Kanehisa, M., Goto, S., and Ogata, H.  
484 (2020) KofamKOALA: KEGG Ortholog assignment based on profile HMM and adaptive score  
485 threshold. *Bioinformatics* **36**: 2251–2252.
- 486 Bissett, A., Fitzgerald, A., Meintjes, T., Mele, P.M., Reith, F., Dennis, P.G., et al. (2016)  
487 Introducing BASE: the Biomes of Australian Soil Environments soil microbial diversity  
488 database. *GigaScience* **5**: 21.

- 489 Bowers, R.M., Kyrpides, N.C., Stepanauskas, R., Harmon-Smith, M., Doud, D., Reddy, T.B.K.,  
490 et al. (2017) Minimum information about a single amplified genome (MISAG) and a  
491 metagenome-assembled genome (MIMAG) of bacteria and archaea. *Nat Biotechnol* **35**: 725–731.
- 492 Bowman, J.P. (2013) Sea-Ice Microbial Communities. In *The Prokaryotes*. Rosenberg, E.,  
493 DeLong, E.F., Lory, S., Stackebrandt, E., and Thompson, F. (eds). Berlin, Heidelberg: Springer  
494 Berlin Heidelberg, pp. 139–161.
- 495 Buchfink, B., Xie, C., and Huson, D.H. (2015) Fast and sensitive protein alignment using  
496 DIAMOND. *Nat Methods* **12**: 59–60.
- 497 Butterbach-Bahl, K., Baggs, E.M., Dannenmann, M., Kiese, R., and Zechmeister-Boltenstern,  
498 S. (2013) Nitrous oxide emissions from soils: how well do we understand the processes and their  
499 controls? *Philos Trans R Soc B Biol Sci* **368**: 20130122.
- 500 Camacho, C., Coulouris, G., Avagyan, V., Ma, N., Papadopoulos, J., Bealer, K., and Madden,  
501 T.L. (2009) BLAST+: architecture and applications. *BMC Bioinformatics* **10**: 421.
- 502 Cavicchioli, R. (2006) Cold-adapted archaea. *Nat Rev Microbiol* **4**: 331–343.
- 503 Chauhan, A., Layton, A.C., Vishnivetskaya, T.A., Williams, D., Pffiffner, S.M., Rekepalli, B., et  
504 al. (2014) Metagenomes from Thawing Low-Soil-Organic-Carbon Mineral Cryosols and  
505 Permafrost of the Canadian High Arctic. *Genome Announc* **2**:
- 506 Chaumeil, P.-A., Mussig, A.J., Hugenholtz, P., and Parks, D.H. (2019) GTDB-Tk: a toolkit to  
507 classify genomes with the Genome Taxonomy Database. *Bioinformatics* btz848.
- 508 Ciufu, S., Kannan, S., Sharma, S., Badretdin, A., Clark, K., Turner, S., et al. (2018) Using  
509 average nucleotide identity to improve taxonomic assignments in prokaryotic genomes at the  
510 NCBI. *Int J Syst Evol Microbiol* **68**: 2386–2392.
- 511 Daebeler, A., Abell, G.C.J., Bodelier, P.L.E., Bodrossy, L., Frampton, D.M.F., Hefting, M.M.,  
512 and Laanbroek, H.J. (2012) Archaeal dominated ammonia-oxidizing communities in Icelandic  
513 grassland soils are moderately affected by long-term N fertilization and geothermal heating.  
514 *Front Microbiol* **3**:
- 515 Daims, H., Lebedeva, E.V., Pjevac, P., Han, P., Herbold, C., Albertsen, M., et al. (2015) Complete  
516 nitrification by *Nitrospira* bacteria. *Nature* **528**: 504–509.
- 517 Eddy, S.R. (2011) Accelerated Profile HMM Searches. *PLoS Comput Biol* **7**: e1002195.
- 518 Edgar, R.C. (2004) MUSCLE: multiple sequence alignment with high accuracy and high  
519 throughput. *Nucleic Acids Res* **32**: 1792–1797.



- 520 Edgar, R.C. (2010) Search and clustering orders of magnitude faster than BLAST.  
521 *Bioinformatics* **26**: 2460–2461.
- 522 Eren, A.M., Esen, Ö.C., Quince, C., Vineis, J.H., Morrison, H.G., Sogin, M.L., and Delmont, T.O.  
523 (2015) Anvi'o: an advanced analysis and visualization platform for 'omics data. *PeerJ* **3**: e1319.
- 524 Gadkari, P.S., McGuinness, L.R., Männistö, M.K., Kerkhof, L.J., and Häggblom, M.M. (2020)  
525 Arctic tundra soil bacterial communities active at subzero temperatures detected by stable  
526 isotope probing. *FEMS Microbiol Ecol* **96**: fiz192.
- 527 Galperin, M.Y., Wolf, Y.I., Makarova, K.S., Vera Alvarez, R., Landsman, D., and Koonin, E.V.  
528 (2021) COG database update: focus on microbial diversity, model organisms, and widespread  
529 pathogens. *Nucleic Acids Res* **49**: D274–D281.
- 530 Hayashi, K., Tanabe, Y., Fujitake, N., Kida, M., Wang, Y., Hayatsu, M., and Kudoh, S. (2020)  
531 Ammonia Oxidation Potentials and Ammonia Oxidizers of Lichen–Moss Vegetated Soils at Two  
532 Ice-free Areas in East Antarctica. *Microbes Environ* **35**: n/a.
- 533 Hwang, Y., Schulze-Makuch, D., Arens, F.L., Saenz, J.S., Adam, P.S., Sager, C., et al. (2021)  
534 Leave no stone unturned: individually adapted xerotolerant Thaumarchaeota sheltered below  
535 the boulders of the Atacama Desert hyperarid core. *Microbiome* **9**: 234.
- 536 Hyatt, D., Chen, G.-L., LoCascio, P.F., Land, M.L., Larimer, F.W., and Hauser, L.J. (2010)  
537 Prodigal: prokaryotic gene recognition and translation initiation site identification. *BMC*  
538 *Bioinformatics* **11**: 119.
- 539 Ji, M., Greening, C., Vanwonderghem, I., Carere, C.R., Bay, S.K., Steen, J.A., et al. (2017)  
540 Atmospheric trace gases support primary production in Antarctic desert surface soil. *Nature*  
541 **552**: 400–403.
- 542 Jung, M.-Y., Islam, Md.A., Gwak, J.-H., Kim, J.-G., and Rhee, S.-K. (2018) Nitrosarchaeum  
543 koreense gen. nov., sp. nov., an aerobic and mesophilic, ammonia-oxidizing archaeon member  
544 of the phylum Thaumarchaeota isolated from agricultural soil. *Int J Syst Evol Microbiol* **68**:  
545 3084–3095.
- 546 Jung, M.-Y., Sedlacek, C.J., Kits, K.D., Mueller, A.J., Rhee, S.-K., Hink, L., et al. (2022)  
547 Ammonia-oxidizing archaea possess a wide range of cellular ammonia affinities. *ISME J* **16**:  
548 272–283.
- 549 Katoh, K. and Standley, D.M. (2013) MAFFT Multiple Sequence Alignment Software Version  
550 7: Improvements in Performance and Usability. *Mol Biol Evol* **30**: 772–780.

- 551 Kerou, M., Offre, P., Valledor, L., Abby, S.S., Melcher, M., Nagler, M., et al. (2016) Proteomics  
552 and comparative genomics of *Nitrososphaera viennensis* reveal the core genome and adaptations  
553 of archaeal ammonia oxidizers. *Proc Natl Acad Sci* **113**: E7937–E7946.
- 554 Kim, M., Oh, H.-S., Park, S.-C., and Chun, J. (2014) Towards a taxonomic coherence between  
555 average nucleotide identity and 16S rRNA gene sequence similarity for species demarcation of  
556 prokaryotes. *Int J Syst Evol Microbiol* **64**: 346–351.
- 557 Kits, K.D., Sedlacek, C.J., Lebedeva, E.V., Han, P., Bulaev, A., Pjevac, P., et al. (2017) Kinetic  
558 analysis of a complete nitrifier reveals an oligotrophic lifestyle. *Nature* **549**: 269–272.
- 559 Komárek, J., Kaňtovský, J., Ventura, S., and Turicchia, S. Āmarda (2009) The cyanobacterial  
560 genus *Phormidesmis*. *Algol Stud* **129**: 41–59.
- 561 Könneke, M., Schubert, D.M., Brown, P.C., Hugler, M., Standfest, S., Schwander, T., et al.  
562 (2014) Ammonia-oxidizing archaea use the most energy-efficient aerobic pathway for CO<sub>2</sub>  
563 fixation. *Proc Natl Acad Sci* **111**: 8239–8244.
- 564 Konstantinidis, K.T., Rosselló-Móra, R., and Amann, R. (2017) Uncultivated microbes in need  
565 of their own taxonomy. *ISME J* **11**: 2399–2406.
- 566 Lagkouvardos, I., Joseph, D., Kapfhammer, M., Giritli, S., Horn, M., Haller, D., and Clavel, T.  
567 (2016) IMNGS: A comprehensive open resource of processed 16S rRNA microbial profiles for  
568 ecology and diversity studies. *Sci Rep* **6**: 33721.
- 569 Langmead, B. and Salzberg, S.L. (2012) Fast gapped-read alignment with Bowtie 2. *Nat*  
570 *Methods* **9**: 357–359.
- 571 Lehtovirta-Morley, L.E. (2018) Ammonia oxidation: Ecology, physiology, biochemistry and why  
572 they must all come together. *FEMS Microbiol Lett* **365**:
- 573 Lehtovirta-Morley, L.E., Ross, J., Hink, L., Weber, E.B., Gubry-Rangin, C., Thion, C., et al.  
574 (2016) Isolation of ‘*Candidatus Nitrosocosmicus franklandus*’, a novel ureolytic soil archaeal  
575 ammonia oxidiser with tolerance to high ammonia concentration. *FEMS Microbiol Ecol* **92**:  
576 fiw057.
- 577 Lehtovirta-Morley, L.E., Stoecker, K., Vilcinskis, A., Prosser, J.I., and Nicol, G.W. (2011)  
578 Cultivation of an obligate acidophilic ammonia oxidizer from a nitrifying acid soil. *Proc Natl*  
579 *Acad Sci* **108**: 15892–15897.
- 580 Leininger, S., Urich, T., Schloter, M., Schwark, L., Qi, J., Nicol, G.W., et al. (2006) Archaea  
581 predominate among ammonia-oxidizing prokaryotes in soils. *Nature* **442**: 806–809.

- 582 Li, D., Liu, C.-M., Luo, R., Sadakane, K., and Lam, T.-W. (2015) MEGAHIT: an ultra-fast single-  
583 node solution for large and complex metagenomics assembly via succinct de Bruijn graph.  
584 *Bioinformatics* **31**: 1674–1676.
- 585 Li, H. (2016) Minimap and miniasm: fast mapping and de novo assembly for noisy long  
586 sequences. *Bioinformatics* **32**: 2103–2110.
- 587 Li, H., Handsaker, B., Wysoker, A., Fennell, T., Ruan, J., Homer, N., et al. (2009) The Sequence  
588 Alignment/Map format and SAMtools. *Bioinformatics* **25**: 2078–2079.
- 589 Magalhães, C.M., Machado, A., Frank-Fahle, B., Lee, C.K., and Cary, S.C. (2014) The ecological  
590 dichotomy of ammonia-oxidizing archaea and bacteria in the hyper-arid soils of the Antarctic  
591 Dry Valleys. *Front Microbiol* **5**.
- 592 Makarova, K., Wolf, Y., and Koonin, E. (2015) Archaeal Clusters of Orthologous Genes  
593 (arCOGs): An Update and Application for Analysis of Shared Features between Thermococcales,  
594 Methanococcales, and Methanobacteriales. *Life* **5**: 818–840.
- 595 Martens-Habbena, W., Berube, P.M., Urakawa, H., de la Torre, J.R., and Stahl, D.A. (2009)  
596 Ammonia oxidation kinetics determine niche separation of nitrifying Archaea and Bacteria.  
597 *Nature* **461**: 976–979.
- 598 Martin, M. (2011) Cutadapt removes adapter sequences from high-throughput sequencing  
599 reads. *EMBnet.journal* **17**: 10.
- 600 Mistry, J., Chuguransky, S., Williams, L., Qureshi, M., Salazar, G.A., Sonnhammer, E.L.L., et  
601 al. (2021) Pfam: The protein families database in 2021. *Nucleic Acids Res* **49**: D412–D419.
- 602 Mussmann, M., Brito, I., Pitcher, A., Sinnighe Damste, J.S., Hatzenpichler, R., Richter, A., et  
603 al. (2011) Thaumarchaeotes abundant in refinery nitrifying sludges express amoA but are not  
604 obligate autotrophic ammonia oxidizers. *Proc Natl Acad Sci* **108**: 16771–16776.
- 605 Nguyen, L.-T., Schmidt, H.A., von Haeseler, A., and Minh, B.Q. (2015) IQ-TREE: A Fast and  
606 Effective Stochastic Algorithm for Estimating Maximum-Likelihood Phylogenies. *Mol Biol Evol*  
607 **32**: 268–274.
- 608 O’Leary, N.A., Wright, M.W., Brister, J.R., Ciufu, S., Haddad, D., McVeigh, R., et al. (2016)  
609 Reference sequence (RefSeq) database at NCBI: current status, taxonomic expansion, and  
610 functional annotation. *Nucleic Acids Res* **44**: D733–D745.
- 611 Ortiz, M., Bosch, J., Coclet, C., Johnson, J., Lebre, P., Salawu-Rotimi, A., et al. (2020) Microbial  
612 Nitrogen Cycling in Antarctic Soils. *Microorganisms* **8**: 1442.

- 613 Parks, D.H., Chuvochina, M., Chaumeil, P.-A., Rinke, C., Mussig, A.J., and Hugenholtz, P.  
614 (2020) A complete domain-to-species taxonomy for Bacteria and Archaea. *Nat Biotechnol*.
- 615 Parks, D.H., Chuvochina, M., Waite, D.W., Rinke, C., Skarszewski, A., Chaumeil, P.-A., and  
616 Hugenholtz, P. (2018) A standardized bacterial taxonomy based on genome phylogeny  
617 substantially revises the tree of life. *Nat Biotechnol* **36**: 996–1004.
- 618 Parks, D.H., Rinke, C., Chuvochina, M., Chaumeil, P.-A., Woodcroft, B.J., Evans, P.N., et al.  
619 (2017) Recovery of nearly 8,000 metagenome-assembled genomes substantially expands the tree  
620 of life. *Nat Microbiol* **2**: 1533–1542.
- 621 Pessi, I.S., Osorio-Forero, C., Gálvez, E.J.C., Simões, F.L., Simões, J.C., Junca, H., and Macedo,  
622 A.J. (2015) Distinct composition signatures of archaeal and bacterial phylotypes in the Wanda  
623 Glacier forefield, Antarctic Peninsula. *FEMS Microbiol Ecol* **91**: 1–10.
- 624 Pessi, I.S., Viitamäki, S., Virkkala, A.-M., Eronen-Rasimus, E., Delmont, T.O., Marushchak,  
625 M.E., et al. (2022) Truncated denitrifiers dominate the denitrification pathway in tundra soil  
626 metagenomes. *bioRxiv*.
- 627 Pester, M., Schleper, C., and Wagner, M. (2011) The Thaumarchaeota: an emerging view of their  
628 phylogeny and ecophysiology. *Curr Opin Microbiol* **14**: 300–306.
- 629 Pritchard, L., Glover, R.H., Humphris, S., Elphinstone, J.G., and Toth, I.K. (2016) Genomics  
630 and taxonomy in diagnostics for food security: soft-rotting enterobacterial plant pathogens. *Anal*  
631 *Methods* **8**: 12–24.
- 632 Qin, W., Heal, K.R., Ramdasi, R., Kobelt, J.N., Martens-Habbena, W., Bertagnolli, A.D., et al.  
633 (2017) *Nitrosopumilus maritimus* gen. nov., sp. nov., *Nitrosopumilus cobalaminigenes* sp. nov.,  
634 *Nitrosopumilus oxyclineae* sp. nov., and *Nitrosopumilus ureiphilus* sp. nov., four marine  
635 ammonia-oxidizing archaea of the phylum Thaumarchaeota. *Int J Syst Evol Microbiol* **67**: 5067–  
636 5079.
- 637 Raymond-Bouchard, I., Goordial, J., Zolotarov, Y., Ronholm, J., Stromvik, M., Bakermans, C.,  
638 and Whyte, L.G. (2018) Conserved genomic and amino acid traits of cold adaptation in subzero-  
639 growing Arctic permafrost bacteria. *FEMS Microbiol Ecol* **94**:
- 640 Richter, I., Herbold, C.W., Lee, C.K., McDonald, I.R., Barrett, J.E., and Cary, S.C. (2014)  
641 Influence of soil properties on archaeal diversity and distribution in the McMurdo Dry Valleys,  
642 Antarctica. *FEMS Microbiol Ecol* **89**: 347–359.

- 643 Rinke, C., Chuvochina, M., Mussig, A.J., Chaumeil, P.-A., Davín, A.A., Waite, D.W., et al. (2021)  
644 A standardized archaeal taxonomy for the Genome Taxonomy Database. *Nat Microbiol* **6**: 946–  
645 959.
- 646 Rosselló-Móra, R. and Amann, R. (2015) Past and future species definitions for Bacteria and  
647 Archaea. *Syst Appl Microbiol* **38**: 209–216.
- 648 Schleper, C. and Nicol, G.W. (2010) Ammonia-Oxidising Archaea – Physiology, Ecology and  
649 Evolution. In *Advances in Microbial Physiology*. Elsevier, pp. 1–41.
- 650 Schloss, P.D. (2021) Amplicon Sequence Variants Artificially Split Bacterial Genomes into  
651 Separate Clusters. *mSphere* **6**: e00191-21.
- 652 Shaiber, A., Willis, A.D., Delmont, T.O., Roux, S., Chen, L.-X., Schmid, A.C., et al. (2020)  
653 Functional and genetic markers of niche partitioning among enigmatic members of the human  
654 oral microbiome. *Genome Biol* **21**: 292.
- 655 Siljanen, H.M.P., Alves, R.J.E., Ronkainen, J.G., Lamprecht, R.E., Bhattarai, H.R., Bagnoud,  
656 A., et al. (2019) Archaeal nitrification is a key driver of high nitrous oxide emissions from arctic  
657 peatlands. *Soil Biol Biochem* **137**: 107539.
- 658 Spang, A., Poehlein, A., Offre, P., Zumbärgel, S., Haider, S., Rychlik, N., et al. (2012) The  
659 genome of the ammonia-oxidizing *Candidatus* Nitrososphaera gargensis: insights into  
660 metabolic versatility and environmental adaptations: The genome of *Candidatus*  
661 Nitrososphaera gargensis. *Environ Microbiol* **14**: 3122–3145.
- 662 Stackebrandt, E. and Ebers, J. (2006) Taxonomic parameters revisited: tarnished gold  
663 standards. *Microbiol Today* **33**: 152–155.
- 664 Stackhouse, B.T., Vishnivetskaya, T.A., Layton, A., Chauhan, A., Pfiffner, S., Mykytczuk, N.C.,  
665 et al. (2015) Effects of simulated spring thaw of permafrost from mineral cryosol on CO<sub>2</sub>  
666 emissions and atmospheric CH<sub>4</sub> uptake. *J Geophys Res Biogeosciences* **120**: 1764–1784.
- 667 Stieglmeier, M., Klingl, A., Alves, R.J.E., Rittmann, S.K.-M.R., Melcher, M., Leisch, N., and  
668 Schleper, C. (2014) Nitrososphaera viennensis gen. nov., sp. nov., an aerobic and mesophilic,  
669 ammonia-oxidizing archaeon from soil and a member of the archaeal phylum Thaumarchaeota.  
670 *Int J Syst Evol Microbiol* **64**: 2738–2752.
- 671 Strunecky, O., Raabova, L., Bernardova, A., Ivanova, A.P., Semanova, A., Crossley, J., and  
672 Kaftan, D. (2020) Diversity of cyanobacteria at the Alaska North Slope with description of two  
673 new genera: Gibliniella and Shackletoniella. *FEMS Microbiol Ecol* **96**: fuz189.



- 674 Tahon, G., Geesink, P., and Ettema, T.J.G. (2021) Expanding Archaeal Diversity and  
675 Phylogeny: Past, Present, and Future. *Annu Rev Microbiol* **75**: 359–381.
- 676 The UniProt Consortium (2019) UniProt: a worldwide hub of protein knowledge. *Nucleic Acids*  
677 *Res* **47**: D506–D515.
- 678 de la Torre, J.R., Walker, C.B., Ingalls, A.E., Könneke, M., and Stahl, D.A. (2008) Cultivation  
679 of a thermophilic ammonia oxidizing archaeon synthesizing crenarchaeol. *Environ Microbiol* **10**:  
680 810–818.
- 681 Voigt, C., Marushchak, M.E., Abbott, B.W., Biasi, C., Elberling, B., Siciliano, S.D., et al. (2020)  
682 Nitrous oxide emissions from permafrost-affected soils. *Nat Rev Earth Environ* **1**: 420–434.
- 683 Wang, Q., Zhu, R., Zheng, Y., Bao, T., and Hou, L. (2019) Effects of sea animal colonization on  
684 the coupling between dynamics and activity of soil ammonia-oxidizing bacteria and archaea in  
685 maritime Antarctica. *Biogeosciences* **16**: 4113–4128.
- 686 Wu, L., Chen, X., Wei, W., Liu, Y., Wang, D., and Ni, B.-J. (2020) A Critical Review on Nitrous  
687 Oxide Production by Ammonia-Oxidizing Archaea. *Environ Sci Technol* **54**: 9175–9190.
- 688 Xie, Z., Le Roux, X., Wang, C., Gu, Z., An, M., Nan, H., et al. (2014) Identifying response groups  
689 of soil nitrifiers and denitrifiers to grazing and associated soil environmental drivers in Tibetan  
690 alpine meadows. *Soil Biol Biochem* **77**: 89–99.
- 691 Yang, Y., Zhang, C., Lenton, T.M., Yan, X., Zhu, M., Zhou, M., et al. (2021) The Evolution  
692 Pathway of Ammonia-Oxidizing Archaea Shaped by Major Geological Events. *Mol Biol Evol* **38**:  
693 3637–3648.
- 694 Yarza, P., Yilmaz, P., Pruesse, E., Glöckner, F.O., Ludwig, W., Schleifer, K.-H., et al. (2014)  
695 Uniting the classification of cultured and uncultured bacteria and archaea using 16S rRNA gene  
696 sequences. *Nat Rev Microbiol* **12**: 635–645.
- 697 Zhang, S., Xia, X., Li, S., Zhang, L., Wang, G., Li, M., et al. (2019) Ammonia Oxidizers in High-  
698 Elevation Rivers of the Qinghai-Tibet Plateau Display Distinctive Distribution Patterns. *Appl*  
699 *Environ Microbiol* **85**.

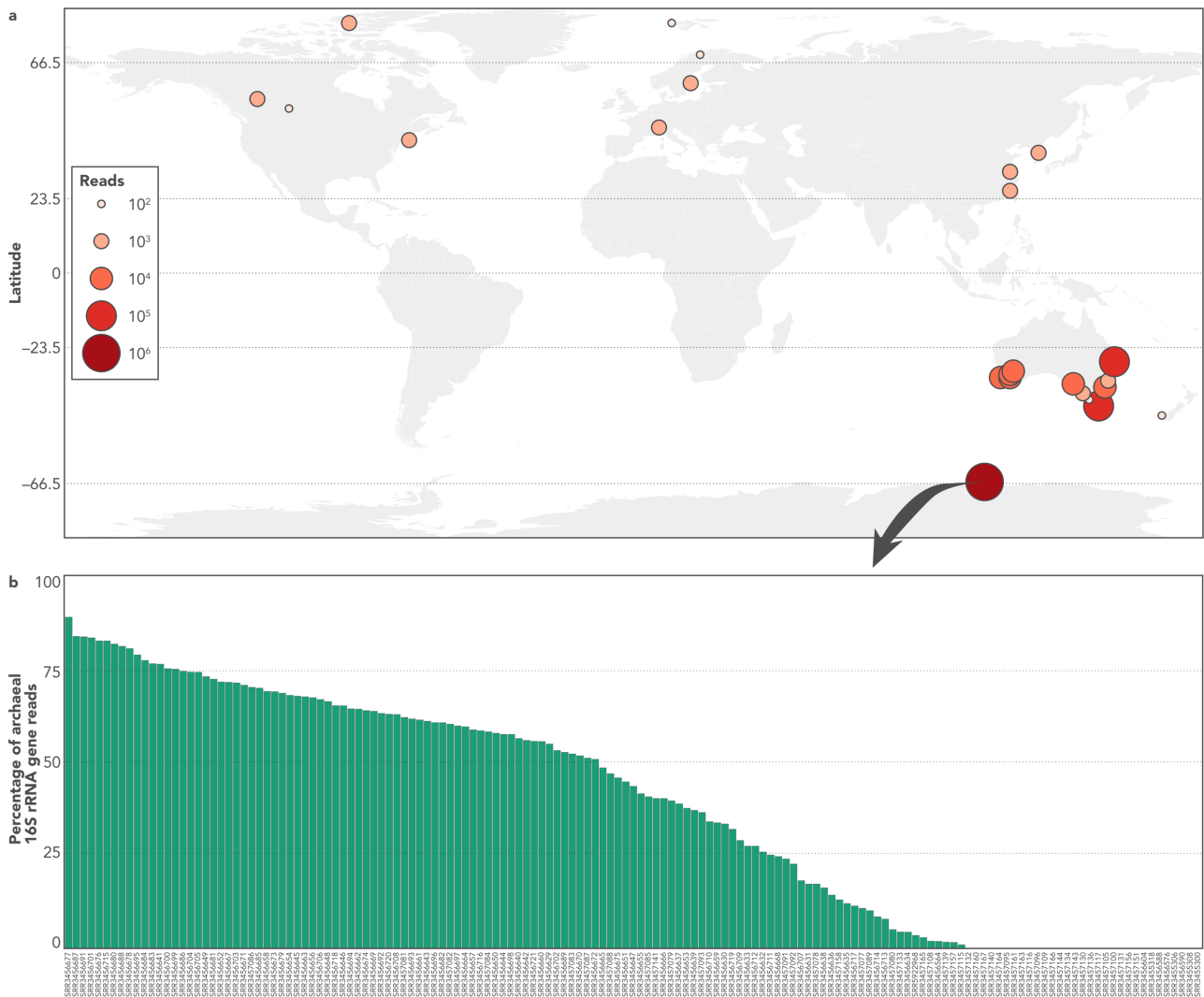
700 **SSupplementary Information**

701 **Suppl. Table S1 (separate .xlsx file).** Additional information on metagenome-assembled  
702 genomes (MAGs) belonging to the UBA10452 lineage (*Candidatus Nitrosopolaris*).

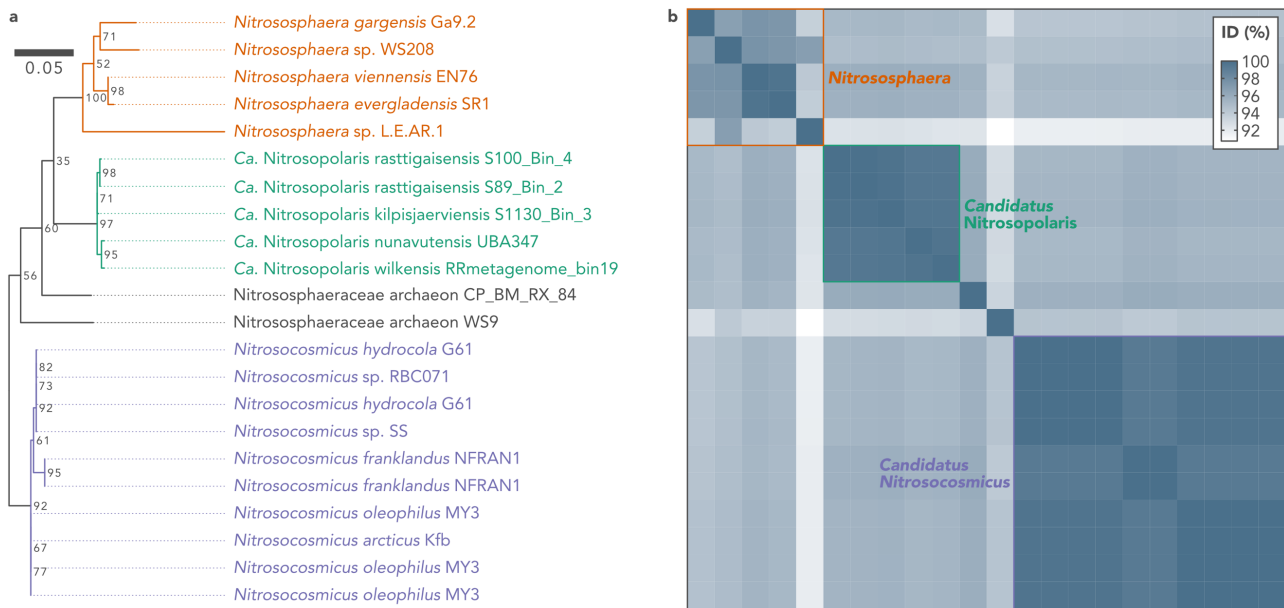
703 **Suppl. Table S2 (separate .xlsx file).** Information about selected genes used for the  
704 reconstruction of the metabolic potential of the UBA10452 lineage (*Candidatus Nitrosopolaris*).

705 **Suppl. Table S3 (separate .xlsx file).** arCOG functions enriched in metagenome-assembled  
706 genomes (MAGs) belonging to the UBA10452 lineage (*Candidatus Nitrosopolaris*).

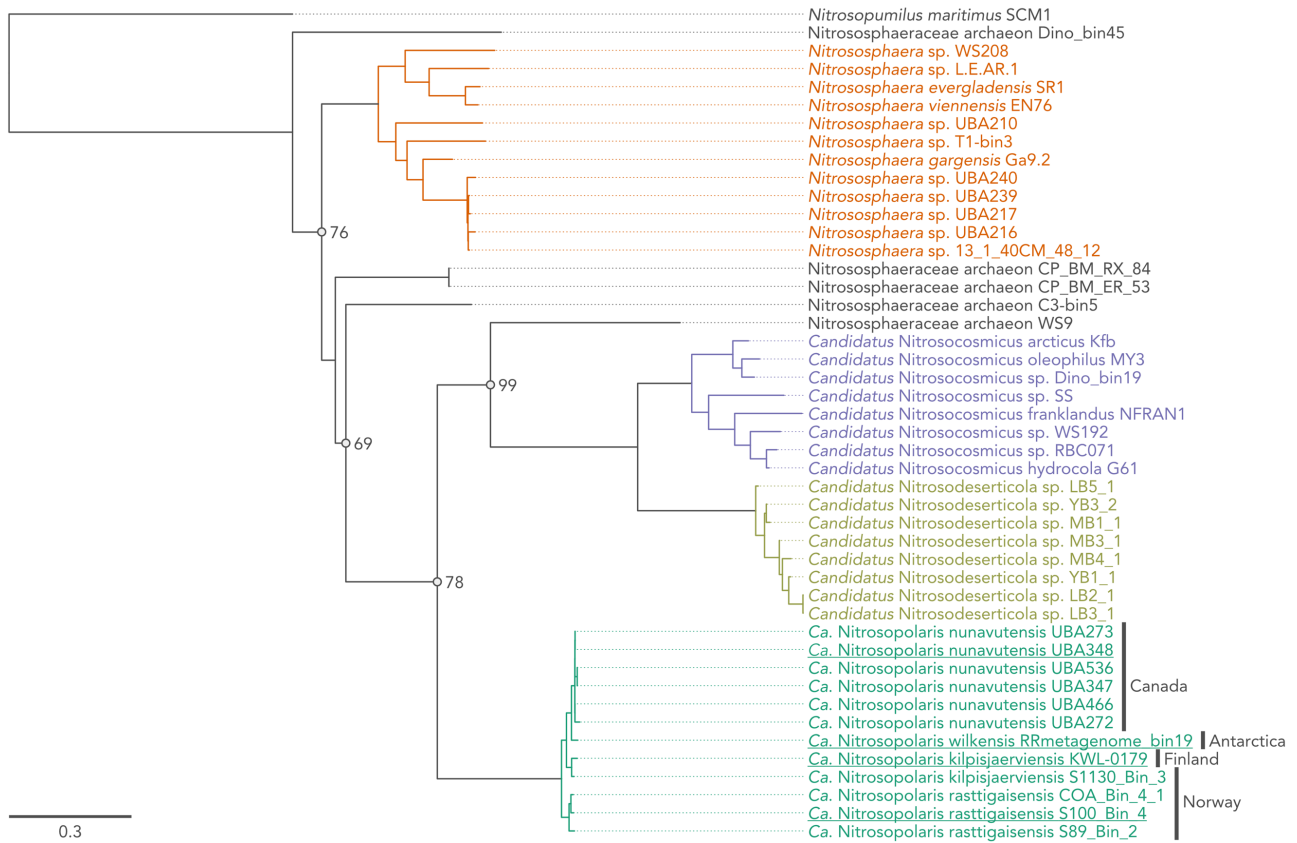
707 **Suppl. Table S4 (separate .xlsx file).** Genes with known or predicted roles in cold adaptation  
708 and growth found in metagenome-assembled genomes (MAGs) belonging to the UBA10452  
709 lineage (*Candidatus Nitrosopolaris*).



710 **Suppl. Figure S1. Geographic distribution of the UBA10452 lineage (*Candidatus***  
711 ***Nitrosopolaris*).** **a)** Distribution of *Ca. Nitrosopolaris* based on the screening of 422,877 16S  
712 rRNA gene amplicon sequencing datasets in the Sequence Read Archive (SRA). Datasets with  
713 few matches (< 0.1% or < 100 reads) are not shown. **b)** Abundance of *Ca. Nitrosopolaris* across  
714 149 16S rRNA gene amplicon sequencing datasets from soils in the vicinity of Davis Station,  
715 Princess Elizabeth Land, Antarctica (BioProject PRJNA317932). Relative abundances were  
716 computed as the proportion of reads matching the sequence of *Ca. Nitrosopolaris* in each  
717 sample. Abundances represent the percentage of *Ca. Nitrosopolaris* reads relative to archaeal  
718 16S rRNA gene reads obtained with archaea-specific primers.

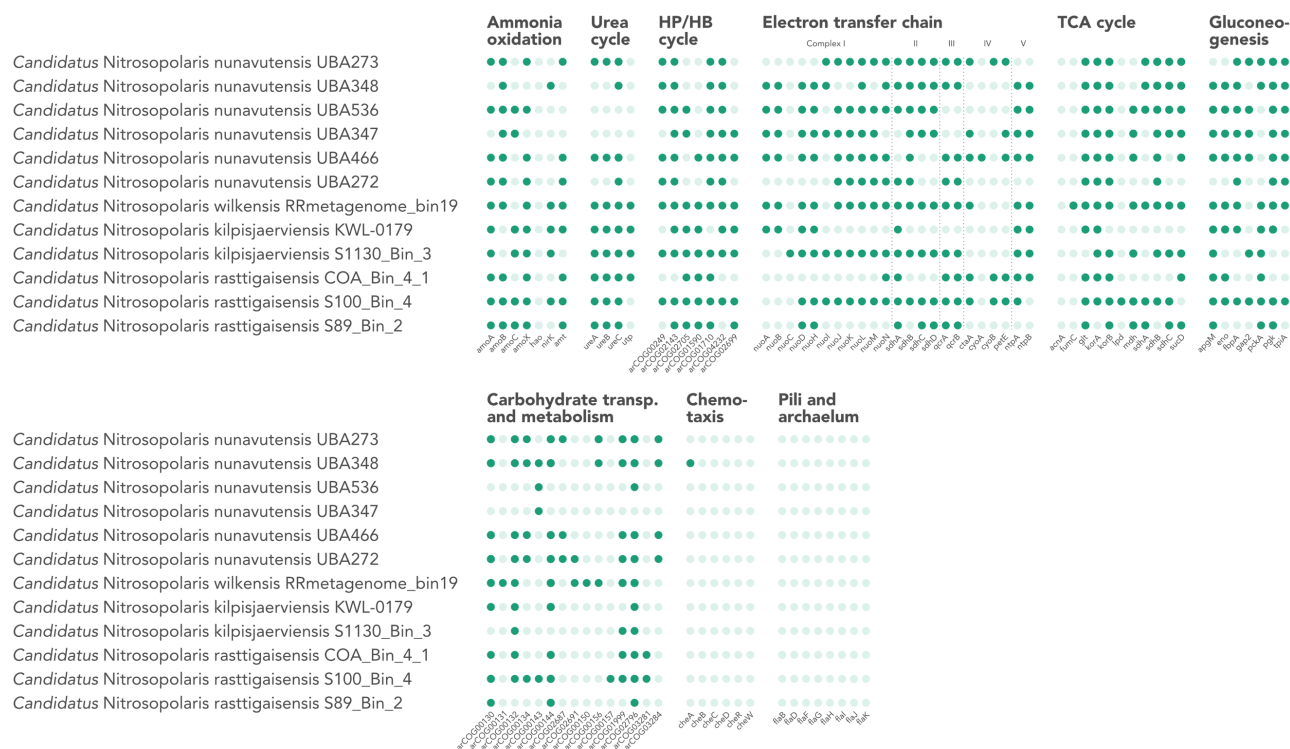


719 **Suppl. Figure S2. The 16S rRNA gene of UBA10452 (*Candidatus Nitrosopolaris*).**  
720 **a)** Phylogenetic analysis of the 16S rRNA gene sequence of five metagenome-assembled  
721 genomes (MAGs) assigned to the UBA10452 lineage and other Nitrososphaeraceae genomes  
722 available on GenBank. Maximum likelihood tree rooted with *Nitrosopumilus maritimus* SCM1  
723 (not shown). Bootstrap values for node support are indicated. **b)** Pairwise similarity between  
724 16S rRNA gene sequences. Note that some genomes contain multiple copies of the 16S rRNA  
725 gene.



726 **Suppl. Figure S3. Phylogenomic analysis of the UBA10452 lineage (*Candidatus***  
 727 ***Nitrosopolaris*).** Maximum likelihood tree based on 59 single-copy genes from 12 metagenome-  
 728 assembled genomes (MAGs) assigned to the UBA10452 lineage and 33 other  
 729 Nitrososphaeraceae genomes available on GenBank. *Nitrosopumilus maritimus* SCM1 was  
 730 used for rooting the tree. Nodes are supported by bootstrap values of 100% unless shown  
 731 otherwise. Representatives for the four proposed species are indicated in underscore. This is an  
 732 uncollapsed and bootstrapped version of the tree found in **Fig. 2a**.





733

**Suppl. Figure S4. Metabolic potential of the UBA10452 lineage (*Candidatus***

734

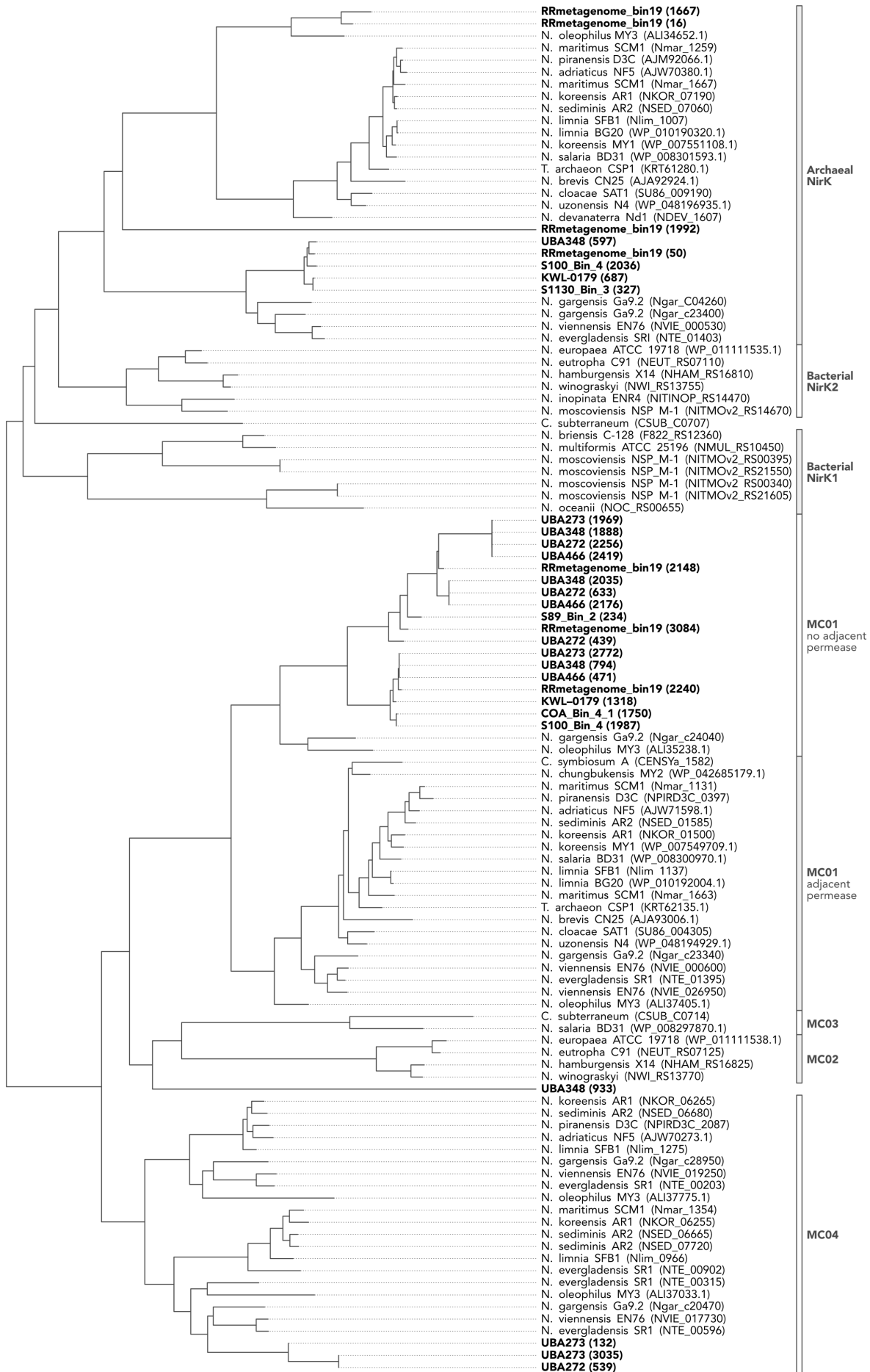
***Nitrosopolaris*). Metabolic potential was estimated based on the presence of key genes**

735

**involved in selected pathways. Detailed information about the genes can be found in Suppl.**

736

**Table S2.**



738 **(Previous page) Suppl. Figure S5. Phylogenetic analysis of putative NirK sequences**  
739 **from metagenome-assembled genomes (MAGs) belonging to the UBA10452 lineage**  
740 **(*Candidatus Nitrosopolaris*).** Sequences from the UBA10452 are shown in bold and  
741 respective gene calls are given inside parenthesis. Other sequences were retrieved from Kerou  
742 *et al.* (2016).